Inorg. Chem. **2004**, *43*, 189–197

Anionic Platinum Complexes with 2-Pyridylphosphines as Ligands for Rhodium: Synthesis of Zwitterionic Pt–Rh Organometallic Compounds

Juan A. Casares, Pablo Espinet,* José M. Martín-Alvarez, and Verónica Santos

Química Inorgánica, Facultad de Ciencias, Universidad de Valladolid, E-47005 Valladolid, Spain

Received July 21, 2003

Bimetallic zwitterionic platinum(II)–rhodium(I) complexes of the type $[(C_6F_5)_3Pt(\mu\text{-}PPy_nPh_{3-n})Rh(CO)_2]$ and $[(C_6F_5)_3Pt(\mu\text{-}PPy_nPh_{3-n})Rh(diene))]$ ($n = 2, 3$; Py = 2-pyridyl) have been prepared. The P end of the bridging ligands (μ-PPy_nPh_{3-n}) is always coordinated to the Pt center, while the N-donor ends chelate the Rh atom, giving metallacycles comparable to pyrazolylborate–Rh complexes. These metallacycles can adopt two conformations, either with the Pt complex in pseudoaxial position approaching the Rh center or with the Pt complex in a remote position. The preferred conformation depends on the steric hindrance at the rhodium center. In less sterically demanding Rh–carbonyl complexes the Pt moiety gets close to the Rh moiety as this brings closer the opposite charges of the zwitterion. For diene complexes mixtures of conformers are obtained. The X-ray structures of $[(C_6F_5)_3Pt(\mu\text{-}PPhPy_2)Rh(COD)]$ (COD = 1,5-cyclooctadiene) and $[(C_6F_5)_3Pt(\mu\text{-}PPhPy_2)Rh(CO)_2]$ are reported.

Introduction

The coordination chemistry of the 2-pyridylphosphines is currently a topic of great interest, which has been extensively reviewed.[1] Most studies have been concerned with PPh_2Py (Py = 2-pyridyl). This is a useful building block for the synthesis of homo- or heterobimetallic compounds because the rigidity induced by the small bite angle of the ligand favors the formation of M−M bonds. On the other hand, the different electronic properties for P and N donor atoms facilitate stereoselective bonding of the ligand in molecules with both hard and soft metal centers. The coordination chemistry of tridentate and tetradentate ligands $PPhPy_2$ and PPy_3 has been much less studied, but there are a few reports on their catalytic application as amphiphilic water-soluble ligands and as proton carriers.[2−4]

As a part of our ongoing research on complexes with pyridylphosphines and their derivatives,[4,5] we have studied before homobimetallic complexes with PPy_nPh_{3-n} ($n = 2$, 3) as bridging ligands.[4,6] $PPhPy_2$ and PPy_3 coordinate to the monoanionic moiety "$Pt(C_6F_5)_3$" through the P atom giving $[Pt(C_6F_5)_3(PPy_nPh_{3-n})]^-$. The pendant pyridyl groups can then bind a cationic rhodium center, forming zwitterionic heterobimetallic complexes.[7] The geometry of these compounds makes them comparable to bis- and tris(pyrazolyl)borate complexes (Chart 1),[8] although in $[Pt(C_6F_5)_3(PPy_nPh_{3-n})]^-$

* To whom correspondence should be addressed. E-mail: espinet@qi.uva.es.

(1) (a) Espinet, P.; Soulantica, K. *Coord. Chem. Rev.* **1999**, 499−556. (b) Zhang, Z. Z.; Cheng, H. *Coord. Chem. Rev.* **1996**, *147*, 1−39. (c) Newkome, G. R. *Chem. Rev.* **1993**, *93*, 2067−2089.

(2) (a) Pruchnik, F. P.; Smolenski, P.; Wajda-Hermanowicz, K. *J. Organomet. Chem.* **1998**, *570*, 63−69. (b) Buhling, A.; Kamer, P. C. J.; van Leeuwen, P. W. N. M.; Elgersma, J. W. *J. Mol. Catal. A: Chem.* **1997**, *116*, 297−308. (c) Baird, I. R.; Smith, M. B.; James, B. R. *Inorg. Chim. Acta* **1995**, *235*, 291−297. (d) Buhling, A.; Kamer, P. C. J.; van Leeuwen P. W. N. M. *J. Mol. Catal. A: Chem.* **1995**, *98*, 69−80 (e) Drent, E.; Arnoldy, P.; Budzelaar, P. H. M. *J. Organomet. Chem.* **1993**, *455*, 247. (f) Xie, Y.; Lee, C.-L.; Yang, Y.; Rettig, S. J.; James, B. R. *Can. J. Chem.* **1992**, *70*, 751−756.

(3) (a) Schutte, R. P.; Rettig, S. J.; Joshi, A. J.; James. R. J. *Inorg. Chem.* **1997**, *36*, 5809−5817. (b) Wajda-Hermanowicz, K.; Pruchnik, F.; Zuber, M. *J. Organomet. Chem.* **1996**, *508*, 75−81.

(4) (a) Espinet, P.; Hernando, R.; Iturbe, G.; Villafañe, F.; Orpen, A. G.; Pascual, I. *Eur. J. Inorg. Chem.* **2000**, *5*, 1031−1038. (b) Casares, J. A.; Espinet, P.; Hernando, R.; Iturbe, G.; Villafañe, F. *Inorg. Chem.* **1997**, *36*, 44−49. (c) Espinet, P.; Gómez-Elipe, P.; Villafañe, F. *J. Organomet. Chem.* **1993**, *450*, 145−150.

(5) (a) Alonso, M. A.; Casares, J. A.; Espinet, P.; Martínez-Ilarduya, J. M.; Pérez-Briso, C. *Eur. J. Inorg. Chem.* **1998**, 1745−1753. (b) Casares, J. A.; Espinet, P.; Martínez de Ilarduya, J. M.; Lin, Y.-S. *Organometallics* **1997**, *16*, 770−779. (c) Casares, J. C.; Coco, S.; Espinet, P.; Lin, Y.-S. *Organometallics* **1995**, *14*, 3058−3067. (d) Casares, J. A.; Espinet, P.; Martín-Alvarez, J. M.; Espino, G.; Pérez-Manrique, M.; Vattier, F. *Eur. J. Inorg. Chem.* **2001**, 289−296.

(6) (a) Alonso, M. A.; Casares, J. A.; Espinet, P.; Soulantica, K.; Charmant, J. P. H.; Orpen, A. G. *Inorg. Chem.* **2000**, *39*, 705−711. (b) Casares, J. A.; Espinet, P.; Soulantica, K.; Pascual, I.; Orpen, A. G. *Inorg. Chem.* **1997**, *36*, 5251.

(7) For recent advances in zwitterionic organometallics, see: (a) Betley, T. A.; Peters J. C. *Angew. Chem., Int. Ed.* **2003**, *42*, 2385−2389. (b) Betley T. A.; Peters J. C. *Inorg. Chem.* **2002**, *41*, 6541−6543 and references therein. (c) Lu, C.; Peters, J. C. *J. Am. Chem. Soc.* **2002**, 5272−5273. (d) Viau, L.; Lepetit, C.; Commenges, G.; Chauvin, R. *Organometallics* **2001**, 808−810. (e) Marx, T.; Wesemann, L.; Dehnen, S. *Organometallics* **2000**, 4653−4656. (f) Chauvin, R. *Eur. J. Inorg. Chem.* **2000**, 577−591.

10.1021/ic034863f CCC: $27.50
Published on Web 12/06/2003

Chart 1

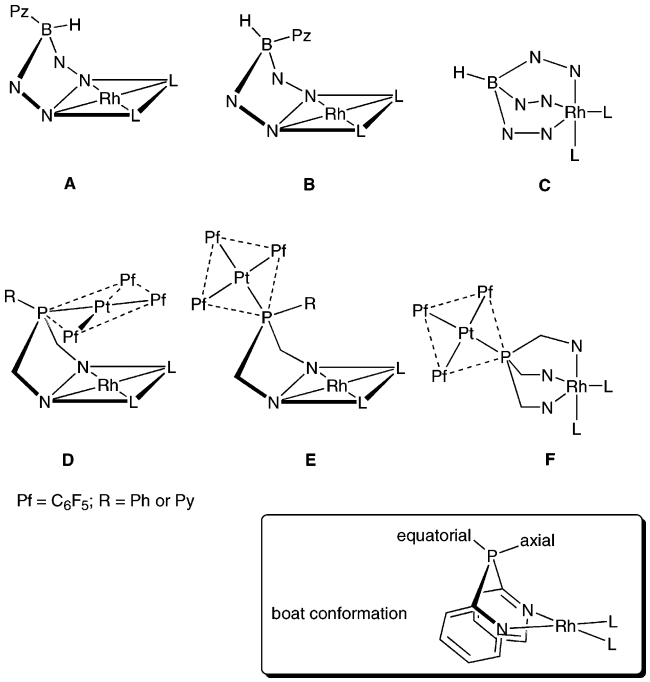

the negative charge is distributed differently from Tp′ ligands (Tp′: hydridotris(pyrazolyl)borate). Formally, the complexes with $[Pt(C_6F_5)_3(PPy_nPh_{3-n})]^-$ have a negative charge at the Pt and a positive charge at the Rh. Although the negative charge at the platinum should be in part delocalized into the perfluoroaryl rings, this charge separation could still influence the stereochemistry of the complexes.

Complexes $MTp'L_2$ (M = Rh(I), Ir(I)) show κ^2 or κ^3 coordination modes depending on the nature of the Tp′ ligand, the metal, and the coligands L. While κ^3 coordination yields 18-electron trigonal-bipyramidal structures (complexes **C** in Chart 1), κ^2 binding results in 16-electron square-planar species. In the latter the different substituents at the boron can be oriented in pseudoequatorial or pseudoaxial positions in the boat defined by the chelate, giving rise to different conformers (**A** or **B** in Chart 1). These aspects, well studied in pyrazolylborate chemistry,[6,9] are examined here for the complexes with the ligands $[Pt(C_6F_5)_3(PPy_nPh_{3-n})]^-$, where similar structures (**D**−**F**) might appear, but other forces such as the charge on the metals and the bulk of $[Pt(C_6F_5)_3(PPy_nPh_{3-n})]^-$ are involved.

Experimental Section

General Methods. All reactions were carried out under N_2. Solvents were distilled using standard methods. The compounds $[Rh_2(\mu\text{-Cl})_2(1,5\text{-COD})_2]$,[10] $[Rh_2(\mu\text{-Cl})_2(TFB)_2]$,[11] $[Rh_2(\mu\text{-Cl})_2(CO)_4]$,[12] $PPhPy_2$,[13] PPy_3,[14] and $(NBu_4)[Pt(C_6F_5)_3(tht)]$[15] (TFB = 5,6,7,8-tetrafuoro-1,4-dihydro-1,4-etenonaphthalene, trivial name tetrafluorobenzobarrelene; tht = tetrahydrothiophene) were prepared by published methods. Combustion CHN analyses were done on a Perkin-Elmer 2400 CHN microanalyzer. IR spectra were recorded on a Perkin-Elmer FT 1720 X spectrophotometer.

NMR Spectra. ^1H NMR (300.16 MHz), ^{19}F NMR (282.4 MHz), ^{31}P NMR (121.4 MHz), and ^{195}Pt NMR (64.2 MHz) spectra were recorded on Bruker ARX 300 and AC 300 instruments equipped with a VT-100 variable-temperature probe. Chemical shifts are reported in ppm from $SiMe_4$ (^1H), CCl_3F (^{19}F), H_3PO_4 (85%) (^{31}P), or $K_2[PtCl_4]$ (1M, D_2O) (^{195}Pt), with positive shifts downfield, at ambient probe temperature unless otherwise stated. *J* values are given in Hz. The $^{19}F-^{195}Pt$ correlation experiments were made operating in inverse mode, with a HMQC sequence with BIRD selection without decoupling during acquisition (in the F_1 projection (^{195}Pt) the signals appear as doublets due to coupling to phosphorus). ^{13}C NMR were registered as $^1H-^{13}C$ correlation experiments, which were made with a HMQC sequence with BIRD selection and GARP decoupling during acquisition. Chemical shifts of quaternary carbons are not listed in the experimental data.

Synthesis of the Complexes. $(NBu_4)[Pt(C_6F_5)_3(PPhPy_2)]$ (1). To a stirred suspension of $(NBu_4)[Pt(C_6F_5)_3(tht)]$ (1.30 g; 1.26 mmol) in EtOH (100 mL) was added $PPhPy_2$ (400.0 mg, 1.52 mmol). The mixture was refluxed for 2 h, the solution was filtered, and the solvent was removed under reduced pressure. The resulting oil was washed twice with *n*-hexane (10 mL) and stirred with EtOH until crystallization of the product as a white solid, which was filtered out, washed with *n*-hexane, and vacuum-dried. Yield: 1.09 g (72%). Anal. Calcd for $C_{50}H_{49}F_{15}N_3PPt$: C, 49.92; H, 4.11; N, 3.49. Found: C, 49.83; H, 4.08; N, 3.33. ^1H NMR (25 °C, $(CD_3)_2CO$, δ): 8.45 (d, 2H); 7.95 (m, 2H); 7.85 (m, 2H); 7.60 (m, 2H); 7.25 (m, 5H); 3.45 (m, 8H); 1.85 (m, 8H); 1.45 (m, 8H); 1.00 (m, 12H). ^{31}P NMR (25 °C, $(CD_3)_2CO$, δ): 16.77, ($^1J_{Pt-P} = 2565$). ^{19}F NMR (25 °C, $(CD_3)_2CO$, δ): −167.5 (m, 2F); −166.5 (m, 6F); −165.5 (m, 1F); −114.0 (m, 2F); −114.9 (m, 4F). ^{195}Pt NMR (25 °C, $(CD_3)_2CO$, δ): − 4369 ($^1J_{Pt-P} = 2642$).

$(NBu_4)[Pt(C_6F_5)_3(PPy_3)]$ (2). It was prepared as described for **1** but using 401.5 mg of PPy_3 (1.52 mmol) instead of $PPhPy_2$. Yield: 1.20 g (81%). Anal. Calcd for $C_{49}H_{48}F_{15}N_4PPt$: C, 48.88; H, 4.02; N, 4.65. Found: C, 48.71; H, 3.96; N, 4.49. ^1H NMR (25 °C, $(CD_3)_2CO$, δ): 8.37 (d, 3H, H-6-Py); 8.20 (m, 3H, H-5-Py); 7.66 (m, 3H, H-4-Py); 7.21 (m, 3H, H-3-Py); 3.46 (m, 8H, NBu_4); 1.85 (m, 8H, NBu_4); 1.44 (m, 8H, NBu_4); 0.97 (m, 12H, NBu_4). ^{31}P NMR (25 °C, $(CD_3)_2CO$, δ): 19.00 ($^2J_{Pt-P} = 2658.6$). ^{19}F NMR (25 °C, $(CD_3)_2CO$, δ): −167.0 (m, 2F); −166.5 (m, 5F); −165.5 (m, 2F); −115.4 (m, 2F); −114.7 (m, 2F); −114.9 (m, 2F). ^{195}Pt NMR (25 °C, $(CD_3)_2CO$, δ): −4373 (d).

$[(C_6F_5)_3Pt(\mu\text{-}PPhPy_2)Rh(CO)_2]$ (3). To a stirred suspension of $AgNO_3$ (42.5 mg; 0.250 mmol) in acetone (15 mL) was added $[Rh(\mu\text{-Cl})(CO)_2]_2$ (48.6 mg, 0.125 mmol). After 30 min of stirring, $(NBu_4)[Pt(C_6F_5)_3(PPhPy_2)]$ (300.7 mg; 0.250 mmol) was added and the mixture was stirred for a further 10 min. The AgCl formed was filtered through Celite, and the yellow solution was evaporated to dryness. The solid residue was purified by column chromatography on silica gel, using CH_2Cl_2 as eluent. Yield: 45% (126.0

(8) (a) Trofimenko, S. *Chem. Rev.* **1993**, *93*, 943−980. (b) Kitajima, N.; Tolman, W. B. *Prog. Inorg. Chem.* **1995**, *43*, 419−531. (c) Slugovc, C.; Padilla-Martínez, I.; Sirol, S.; Carmona, E. *Coord. Chem. Rev.* **2001**, *213*, 129−157.
(9) (a) Bucher, U. E.; Currao, A.; Nesper, R.; Rüeger, H.; Venanzi, L. M.; Younger, E. *Inorg. Chem.* **1995**, *34*, 66−74. (b) Sanz, D.; Santa-María M. D.; Claramunt, R. M.; Cano, M.; Heras, J. V.; Campo, J. A.; Ruíz, F. A.; Pinilla, E.; Monge, A. *J. Organomet. Chem.* **1996**, *526*, 341−350.
(10) Giordano, G.; Crabtree, R. H. *Inorg. Synth.* **1990**, *28*, 88.
(11) Roe, D. M.; Massey A. G. *J. Organomet. Chem.* **1971**, *28*, 273.
(12) Cleverty, M.; Wilkinson, G. *Inorg. Synth.* **1990**, *28*, 84.
(13) (a) Newcome, G.; Hagen, D. C. *J. Org. Chem.* **1978**, *43*, 947−949. (b) Xie, Y.; Lee, C.; Yang, Y.; Rettig, S. J.; James, B. R. *Can. J. Chem.* **1992**, *70*, 751.
(14) Kurtev, K.; Ribola, D.; Jones, R. A.; Cole-Hamilton, D. J.; Wilkinson, G. *J. Chem. Soc., Dalton. Trans.* **1980**, 55−58.
(15) Usón, R.; Forniés, J.; Espinet, P.; Navarro, R.; Martínez, F. *J. Chem. Soc., Chem. Commun*. **1977**, 789.

mg). Anal. Calcd for $C_{36}H_{13}F_{15}N_2O_2PPtRh$: C, 38.60; H, 1.17; N, 2.50. Found: C, 38.79, H, 1.56; N, 2.47. ^{1}H NMR (25 °C, $(CD_3)_2CO$, δ): 9.29 (d, 2H); 8.50 (very broad); 8.02 (m, 2H); 7.86 (d, 1H); 7.70 (m, 4H); 7.23 (m, 2H). ^{31}P{^{1}H} NMR (25 °C, $(CD_3)_2CO$, δ): 20.78 ($^1J_{Pt-P}$ = 2513.6 Hz). ^{19}F NMR (25 °C, $(CD_3)_2CO$, δ): −110.53 (m, 2F, $^3J_{Pt-F}$ = 325); −111.66 (m, 2F, $^3J_{Pt-F}$ = 296); −115.12 (m, 1F, $^3J_{Pt-F}$ = 361); −116.52 (m, 1F, $^3J_{Pt-F}$ = 428); −163.98 (m, 2F); −164.80 (m, 1F); −165.27 (m, 4F); −166.10 (m, 2F). ^{13}C NMR ($(CD_3)_2CO$, δ): 156.6; 142.4; 140.6; 135.8; 134.5; 131.4; 129.9; 129.7; 126.9. ^{195}Pt NMR (25 °C, $(CD_3)_2CO$, δ): −4320 (d). IR (Nujol mull, cm^{-1}): 2107 m, ν(CO); 2050 m, ν(CO); 1591 m, ν(CN). IR (CH_2Cl_2, cm^{-1}): 2103 s, ν(CO); 2044 s, ν(CO).

[$(C_6F_5)_3$Pt(μ-PPy$_3$)Rh(CO)$_2$] (4). This was prepared as described for **3** but using 301 mg of $(NBu_4)[Pt(C_6F_5)_3(PPy_3)]$ (0.25 mmol) instead of $(NBu_4)[Pt(C_6F_5)_3(PPhPy_2)]$. Yield: 45% (125.1 mg). Anal. Calcd for $C_{35}H_{12}F_{15}N_3O_2PPtRh$: C, 37.50; H, 1.08; N, 3.75. Found: C, 38.17; H, 1.47; N 3.66. ^{1}H NMR (25 °C, $(CD_3)_2CO$, δ): 9.58 (t, 1H); 9.28 (d, 2H); 8.87 (d, 1H); 8.40 (m, 1H); 8.00 (m, 2H); 7.85 (m, 2H); 7.67 (m, 2H); 7.12 (m, 2H). ^{31}P{^{1}H} NMR (25 °C, $(CD_3)_2CO$, δ): 20.54 ($^1J_{Pt-P}$ = 2467). ^{13}C NMR (25 °C, $(CD_3)_2CO$, δ): 156.3; 151.8; 140.0; 138.8; 137.7; 131.9; 127.8; 126.8. ^{19}F NMR (25 °C, $(CD_3)_2CO$, δ): −110.87 (m, 2F, $^3J_{Pt-F}$ = 327); −111.66 (m, 2F, $^3J_{Pt-F}$ = 282); −115.31 (m, 1F, $^3J_{Pt-F}$ = 417); −116.48 (m, 1F, $^3J_{Pt-F}$ = 435); −163.74 (m, 2F); −164.91 (m, 5F); −165.99 (m, 2F). ^{195}Pt NMR (25 °C, $(CD_3)_2CO$, δ): −4314 (d). IR (Nujol mull, cm^{-1}): 1591 m, ν(CN); 1574 m, ν(CN); 2098 m, ν(CO); 2044 m, ν(CO). IR (CH_2Cl_2, cm^{-1}): 2102 s, ν(CO); 2044 s, ν(CO).

[$(C_6F_5)_3$Pt(μ-PPhPy$_2$)Rh(COD)] (5). To a stirred solution of $AgClO_4$ (45.5 mg; 0.219 mmol) in acetone (15 mL) was added [Rh(μ-Cl)(COD)]$_2$ (54.1 mg, 0.109 mmol). After 30 min the AgCl was filtered off, and $(NBu_4)[Pt(C_6F_5)_3(PPhPy_2)]$ (264.0 mg; 0.219 mmol) was added to the yellow solution. The solution was stirred for 10 min, the solvent was removed under reduced pressure, and the residue was dissolved in a mixture of CH_2Cl_2 and EtOH (20 mL, 1:1). After partial evaporation of the solvent the compound crystallized as yellow crystals, which were filtered out and vacuum-dried. The product was further purified by column cromatography using silica gel and CH_2Cl_2 as eluent. Yield: 181 mg (78%). Anal. Calcd for $C_{42}H_{25}F_{15}N_2PPtRh$: C, 43.05; H, 2.15; N, 2.39. Found: C, 43.37; H, 2.52; N, 2.60. ^{1}H NMR (25 °C, $(CD_3)_2CO$, δ): 9.91 (broad, 2H); 9.65 (t, 2H); 9.06 (m, 4H); 8.23 (m, 2H); 7.71 (m, 6H); 7.50 (m, 3H); 7.36 (m, 2H); 7.23 (t, 1H); 7.12 (m, 2H); 6.79 (m, 2H); 6.65 (t, 1H); 4.27 (broad, 6H); 3.26 (broad, 2H); 2.84 (broad, 4H); 2.61 (broad, 2H); 2.12 (broad, 2H); 2.04 (2H); 1.86 (broad, 2H); 1.29 (broad, 2H); 0.99 (broad, 2H). ^{1}H NMR (213 K; mixture of **5D** (41%) and **5E** (59%), δ): 9.84 (broad, 2H, **5D**); 9.55 (m, 2H, **5E**); 9.14 (d, 2H, **5E**); 9.10 (d, 2H, **5D**); 8.31(m, 2H, **5E**); 7.81 (m, 1H, **5D**); 7.78 (m, 2H, **5E**); 7.73 (m, 1H, **5D**); 7.67 (m, 1H, **5E**); 7.55 (m, 2H, **5E**); 7.52 (m, 2H, **5D**); 7.35 (m, 2H, **5D**); 7.26 (m, 1H, **5D**); 7.13 (m, 2H, **5D**); 6.85 (m, broad, 2H, **5E**); 6.77 (m, broad, 1H, **5D**); 4.42 (s, broad, 2H, **5D**); 4.27 (broad, 2H, **5E**); 4.01 (broad, 2H, **5D**); 3.32 (broad, 2H, **5E**); 3.06 (broad, 2H, **5D**); 2.71 (broad, 2H, **5D**); 2.55 (broad, 2H, **5E**); 2.16 (broad, 2H, **5D**); 2.04 (broad, 2H, **5D**) 1.82 (d, 2H, **5E**); 1.25 (d, 2H, **5E**); 0.89 (broad, 2H, **5E**). ^{19}F NMR (193 K, δ): −110.7 (m, 2F, $^3J_{Pt-F}$ = 310, **5D**); −112.7 (m, 2F, $^3J_{Pt-F}$ = 282, **5D**), −114.4 (m, 4F, $^3J_{Pt-F}$ = 424, **5E**); −115.8 (m, 2F, $^3J_{Pt-F}$ = 508, **5E**) −115.8 (m, 1F, $^3J_{Pt-F}$ = 395, **5D**), −116.4 (m, 1F, $^3J_{Pt-F}$ = 423, **5D**) −162.5 to −165.5 (m, 9F **5D** + 9F **5E**). ^{13}C NMR (213 K, $(CD_3)_2CO$, δ): 154.2 (**5E**); 153.0 (**5D**); 143.3 (**5D**); 139.8 (**5E**); 138.0 (**5E**); 137.8 (**5D**); 135.3 (**5D**); 132.8 (**5E**); 132.6 (**5E**); 131.6 (**5D**); 130.8 (**5D**); 129.2 (**5D**); 129.0 (**5D**); 128.0 (**5E**); 126.4 (**5E**); 126.0 (**5D**); 90.6 (**5D**); 89.3 (**5E**); 87.8 (**5D**); 85.6 (**5E**); 31.0 (**5D**); 30.6 (**5D**); 30.3 (**5E**); 28.6 (**5E**). ^{31}P{^{1}H} NMR (25 °C, $(CD_3)_2CO$, δ): 40.64 ($^1J_{Pt-P}$ = 2676, **5E**); 23.41 ($^1J_{Pt-P}$ = 2523, **5D**). ^{195}Pt NMR (δ): −4338 (d, **5D**); −4357 (d, **5E**).

Caution: *$AgClO_4$ is potentially explosive and should be handled with care and in small amounts. $AgNO_3$ can be used instead, as described for complex* **3**.

[$(C_6F_5)_3$Pt(μ-PPhPy$_2$)Rh(TFB)] (6). This was prepared as described for **5** but using 80.1 mg of [Rh(μ-Cl)(TFB)]$_2$ (0.109 mmol) instead of [Rh(μ-Cl)(COD)]$_2$. Yield: 145 mg (52%). Anal. Calcd for $C_{46}H_{19}F_{19}N_2PPtRh$: C, 42.84; H, 1.48; N, 2.17. Found: C, 42.83; H, 1.67; N, 2.23. NMR: At room temperature the signals are in coalescence. ^{1}H NMR (200 K, $(CD_3)_2CO$, mixture of **6D** (64%) and **6E** (36%), δ): 9.57 (m, 2H, **6E**); 9.34 (m, 2H, **6E**); 8.95 (d, 2H, **6E**); 8.86 (d, 2H, **6D**); 8.31 (m, 2H, **6E**); 7.91 (m, 2H, **6E**); 7.87 (m, 2H, **6D**); 7.80 (m, 1H, **2E**); 7.79 (m, 1H, **6D**); 7.74 (2H, **6E**); 7.51 (m, 2H, **6D**); 7.49 (m, 1H, **6D**); 7.46 (m, 1H, **6D**); 7.26 (t, 1H, **6D**); 6.95 (t, 1H, **6D**); 6.85 (m, 2H, **6D**); 6.38 (broad, 1H, **6D**); 6.14 (broad, 1H, **6D**); 5.88 (broad 1H, **6E**); 4.68 (broad, 2H, **6D**); 4.36 (broad 2H, **6E**); 4.32 (broad, 2H, **6D**) 4.08 (broad, 1H, **6E**); 3.52 (broad, 2H, **6E**). ^{13}C NMR (193 K, δ): 154.9 (**6E**); 153.8 (**6D**); 142.8 (**6E**); 138.9 (**6E** + **6E** + **6D**); 135.8 (**6D**); 133.8 (**6E**); 132.5 (**6D**), 131.4 (two signals, **6D**); 129.2 (**6E**); 128.4 (**6E**); 126,6 (**6D**); 67.7 (**6D**); 65.7 (**6D**); 63.5 (**6E**); 41.9 (**6D**); 41.3 (**6D**); 40.0 (**6E**); 39.2 (**6E**); 64.3 (**6E**). ^{19}F NMR (δ): −110.19 (m, $^3J_{Pt-F}$ = 323, 2F, **6D**); −113.98 (m, $^3J_{Pt-F}$ = 282, 4F, **6E**); −115.41 (m, $^3J_{Pt-F}$ = 271, 2F, **6D**); −116.21 (m, $^3J_{Pt-F}$ = 240, 2F, **6E**); −116.46 (m, $^3J_{Pt-F}$ = 198, 1F, **6D**); −116.70 (m, $^3J_{Pt-F}$ = 375, 1F, **6D**); −147.47 (broad, 2F TFB, **6D** + **6E**), −160.32 (broad, 2F TFB, **6D** + **6E**); −162.8 to −165.9 (m, 9F **6D** + 9F **6E**). ^{31}P{^{1}H} NMR (213 K, δ): 36.47 ($^1J_{Pt-P}$ = 2672, **6E**); 22.79 ($^1J_{Pt-P}$ = 2525, **6D**). ^{195}Pt NMR (253 K, $(CD_3)_2CO$, δ): −4333 (d, **6D**); −4423 (d, **6E**). IR (Nujol mull, cm^{-1}): 1588 m, ν(CN).

[$(C_6F_5)_3$Pt(μ-PPy$_3$)Rh(COD)] (7). To a stirred solution of $AgNO_3$ (42.5 mg; 0.250 mmol) in acetone (15 mL) was added [Rh(μ-Cl)(COD)]$_2$ (61.6 mg, 0.125 mmol). After 30 min, the mixture was filtered through Celite, and $(NBu_4)[Pt(C_6F_5)_3(PPhPy_3)]$ (301.0 mg; 0.250 mmol) was added to the solution. The mixture was stirred for 10 min, the solvent was evaporated, and the residue was dissolved in a mixture of CH_2Cl_2 and EtOH (10 mL each). After partial evaporation of the solvent the compound crystallized as yellow crystals, which were filtered out and vacuum-dried. The product was further purified by column chromatography on silica gel using CH_2Cl_2 as eluent. Yield: 62% (181.0 mg). Anal. Calcd for $C_{41}H_{24}F_{15}N_3PPtRh$: C, 41.99; H, 2.06; N, 3.58. Found: C, 41.69; H, 2.09; N, 3.52. ^{1}H NMR (25 °C, $(CD_3)_2CO$, δ): 9.91 (m, 2H); 9.05 (d, 2H); 8.85 (m, 3H); 8.45 (d, 2H); 8.30 (m, 2H); 8.10 (m, 3H); 7.75 (m, 2H); 7.60 (m, 4H); 7.50 (m, 2H); 6.60 (m, 2H); 4.30 (m, 4H); 3.75 (m, 4H); 3.00 (m, 2H); 2.21 (d, 4H); 1.85 (m, 6H); 1.66 (d, 4H). ^{19}F NMR (25 °C, $(CD_3)_2CO$, δ): −165.41 (m, 16F); −163.84 (m, 2F); −115.98 (d, 4F); −113.92 (d, 6F); −110.79 (d, 2F). ^{1}H NMR (193 K, mixture of **7D** (45%) and **7E** (55%), δ): 9.80 (m, 1H, **7D**); 9.60 (m, 1H, **7E**); 9.35 (m, 1H, **7E**); 9.15 (m, 1H, **7E**); 9.12 (m, 2H, **7D**); 9.10 (m, 1H, **7E**); 8.50 (m, 1H **7E** + 1H **7D**); 8.30 (m, 1H **7D** + 1H **7E**); 8.29 (m, 1H, **7E**); 7.80 (m, 2H, **7E**); 7.75 (m, 2H, **7D**); 7.70 (m, 1H **7D** + 1H **7E**); 7.50 (m, 2H, **7D**); 7.50 (m, 1H, **7E**); 7.48 (m, 1H, **7E**); 6.60 (m, 2H, **7D**); 4.40 (br, 2H, **7D** + 1H **7E**); 4.15 (s, 1H, **7E**); 3.98 (s, 2H, **7D**); 3.51 (d, 1H, **7E**); 3.41 (m, 1H, **7E**); 3.00 (s, 2H **7D** + 1H **7E**); 2.65 (m, 1H, **7E**); 2.63 (m, 2H, **7D**); 2.48 (s, 1H, **7E**); 2.18 (m, 2H, **7D**); 1.92 (s, 1H, **7E**); 1.75 (s, 1H, **7E**); 1.36 (m, 1H, **7E**); 1.32 (m, 2H, **7D**) 1.18 (m,1H, **7E**); 0.68 (s, 1H, **7E**). ^{13}C NMR

Table 1. X-ray Data and Data Collection and Refinement Parameters

param	**4D**·0.5hex	**5E**·2$(CD_3)_2CO$
	Crystal Data	
empirical formula	$C_{39}H_{20}F_{15}N_2O_2PPtRh$	$C_{48}H_{25}D_{12}F_{15}N_2O_2PPtRh$
fw	1162.54	1299.84
cryst system	monoclinic	orthorhombic
space group	$P2_1/n$	Pbca
a (Å)	9.811(3)	20.766(4)
b (Å)	20.149(5)	17.801(3)
c (Å)	19.413(5)	25.945(5)
β (deg)	93.522(6)	90
V (Å^3)	3830.4(18)	9591(3)
Z	4	8
D_{calc} (g cm^{-3})	2.016	1.800
abs coeff (mm^{-1})	4.233	3.391
F(000)	2228	5024
cryst size (mm)	0.17 × 0.12 × 0.02	0.12 × 0.08 × 0.04
	Data Collection	
temp (K)	298(2)	298(2)
θ range for data collcn (deg)	1.46−23.29	1.57−23.27
wavelength (Å)	0.710 73 (Mo Kα)	0.710 73 (Mo Kα)
index ranges	$-10 \le h \le 10$, $0 \le k \le 22$, $0 \le l \le 21$	$0 \le h \le 23$, $0 \le k \le 19$, $0 \le l \le 28$
reflcns collcd	18 198	45 162
indpdt reflcns	5509 ($R_{int} = 0.0609$)	6880 ($R_{int} = 0.1352$)
obsd reflcns [$I > 2\sigma(I)$]	4240	3948
completeness to θ (deg)	23.29 (99.8%)	23.27 (99.9%)
	Refinement	
abs corr	SADABS	SADABS
max and min transm	1.000 000 and 0.648 923	1.000 000 and 0.852 165
data/restraints/params	5509/0/551	6880/0/688
goodness-of-fit on F^2	1.006	1.012
final R indices [$I > 2\sigma(I)$]	$R_1 = 0.0354$, $wR_2 = 0.0743$	$R_1 = 0.0411$, $wR_2 = 0.0761$
R indices (all data)	$R_1 = 0.0585$, $wR_2 = 0.0841$	$R_1 = 0.1079$, $wR_2 = 0.1013$
largest diff peak and hole (e Å^{-3})	1.428 and −0.460	0.605 and −0.543

(193 K, δ): 155.2 (**7E**); 154.8 (**7E**); 153.8 (**7D**); 152.0 (**7D**); 150.9 (**7E**); 140.5 (**7E**); 140.0 (**7E**); 138.8 (**7D**); 138.6 (**7D**); 138.3 (**7D**); 138.3 (**7E**); 137.0 (**7E**); 136.7 (**7D**); 136.7 (**7E**); 133.0 (**7D**); 128.6 (**7E**); 128.1 (**7E**); 127.4 (**7E**); 127.0 (**7E**); 125.2 (**7D**); 90.3 (**7E**); 88.8 (**7E**); 88.2 (**7D**); 87.7 (**7D**); 86.2 (**7E**); 84.5 (**7E**); 58.4 (**7E**); 31.3 (**7D**); 30.9 (**7E**); 30.7 (**7E**); 30.6 (**7D**); 30.5 (**7D**); 30.5 (**7E**); 30.4 (**7E**); 29.0 (**7D**); 28.9 (**7E**); 28.5 (**7E**); 28.3 (**7E**). $^{31}P\{^1H\}$ NMR (193 K, δ): 40.76 ($^1J_{Pt-P} = 2652$, **7E**); 26.62 ($^1J_{Pt-P} = 2485$, **7D**). ^{195}Pt NMR (25 °C, $(CD_3)_2CO$, δ): −4362 (d, **7D**); −4410 (d, **7E**). IR (Nujol mull, cm^{-1}): 1590 m, ν(CN); 1572 m, ν(CN).

[$(C_6F_5)_3$Pt(μ-PPy$_3$)Rh(TFB)] (8). This compound was prepared as described for **7** but using 91.2 mg of [Rh(μ-Cl)(TFB)]$_2$ (0.125 mmol) instead of [Rh(μ-Cl)(COD)]$_2$. Yield: 40% (129 mg). Anal. Calcd for $C_{45}H_{18}F_{19}N_3PPtRh$: C, 41.88; H, 1.41; N, 3.26. Found: C, 41.81; H, 1.67; N, 3.11. ^1H NMR (25 °C, $(CD_3)_2CO$): At this temperature the signals are in coalescence. ^1H NMR (213 K, mixture of **8D** (65%) and **8E** (35%), δ): 9.64 (broad, 1H, **8D**); 8.82 (m, 1H **8D** + 1H **8E**); 8.69 (d, 1H, **8D**); 8.65 (broad, 3H, **8E**); 8.40 (m, 2H, **8D**); 8.20 (t, 3H, **8E**); 7.78 (m, 2H, **8D** + 1H, **8E**); 7.51 (m, 2H, **8D**); 6.71 (broad, 2H, **8D**); 6.41 (s, 1H **8D**); 6.14 (s, 1H, **8D**); 5.05 (broad, 2H, **8E**); 4.67 (s, 2H, **8D**); 4.37 (s, 2H, **8D**) 3.94 (s, 4H, **8E**). ^{13}C NMR (193 K, $(CD_3)_2CO$, δ): 153.8 (**8D**); 153,5 (**8E**); 152.3 (**8D**); 152.1 (**8E**); 138.9 (**8E**); 138.7 (**8D**); 138.6 (**8D**); 137.6 (**8D**); 132.2 (**8D**); 127.9 (**8D**); 127.5 (**8E**); 126.9 (**8D**); 67.5 (**8D**); 66.0 (**8D**); 64.9 (**8E**); 42.0 (**8D**); 41.4 (**8D**). 40.3 (**8E**). ^{19}F NMR (223 K, $(CD_3)_2CO$, δ): −110.32 (m, 2F, **8D**); −113.64 (m, 4F, **8E**); −115.49 (m, 2F **8D**); −116.46 (m, 2F **8D** + 2F, **8E**); −146.79 (m, 2F-TFB, **8E**); −147.09 (m, 2F-TFB **8D**); −159.64 (m, 2F-TFB, **8E**); −159.78 (m, 2F-TFB **8D**); −163 to −165 (m, 9F **8D** + 9F **8E**). $^{31}P\{^1H\}$ NMR (223 K, δ): 37.24 ($^1J_{Pt-P} = 2642$, **8E**); 25.47 ($^1J_{Pt-P} = 2487$, **8D**). ^{195}Pt NMR: δ −4340 (d, **8D**); −4428 (d, **8E**). IR (Nujol mull, cm^{-1}): 1589 m, ν(CN); 1574 m, ν(CN).

Experimental Procedure for X-ray Crystallography. Suitable single crystals were mounted in glass fibers, and diffraction measurements were made using a Bruker SMART CCD area-detector diffractometer with Mo Kα radiation ($\lambda = 0.710\ 73$ Å).[16] Intensities were integrated from several series of exposures, each exposure covering 0.3° in ω, the total data set being a hemisphere.[17] Absorption corrections were applied, based on multiple and symmetry-equivalent measurements.[18] The structure was solved by direct methods and refined by least squares on weighted F^2 values for all reflections (see Table 1).[19] All non-hydrogen atoms were assigned anisotropic displacement parameters and refined without positional constraints. Hydrogen atoms were taken into account at calculated positions, and their positional parameters were refined. Refinement proceeded smoothly to give $R_1 = 0.0354$ for **4D**·0.5hex (hex = hexane) and $R_1 = 0.0411$ for **5E**·2$(CD_3)_2CO$ on the basis of the reflections with $I > 2\sigma(I)$. Complex neutral-atom scattering factors were used.[20] Crystallographic data (excluding structure factors) for the structures **4D**·0.5hex and **5E**·2$(CD_3)_2CO$ reported in this paper have been deposited with the Cambridge Crystallographic Data Centre as supplementary publications CCDC-200983 and CCDC-202042, respectively. Copies of the data can be obtained free of charge on application to the CCDC, 12 Union Road, Cambridge CB2 1EZ, U.K. [fax (internat.) + 44-1223/336-033; E-mail deposit@ccdc.cam.ac.uk].

(16) *SMART V5.051 Diffractometer Control Software*; Bruker Analytical X-ray Instruments Inc.: Madison, WI, 1998.
(17) *SAINT V6.02 Integration Software*; Bruker Analytical X-ray Instruments Inc.: Madison, WI, 1999.
(18) Sheldrick, G. M. *SADABS: A program for absorption correction with the Siemens SMART system*; University of Göttingen: Göttingen, Germany, 1996.
(19) *SHELXTL program system version 5.1*; Bruker Analytical X-ray Instruments Inc.: Madison, WI, 1998.

Table 2. Selected Spectroscopic Data

compd	isomer (%)	$\delta(^{31}P)$	$\delta(^{13}C)$	$\delta(^{195}Pt)$
$(NBu_4)[Pt(C_6F_5)_3(PPhPy_2)]$ (**1**)		16.7		−4368
$[Pt(C_6F_5)_3](\mu\text{-}PPhPy_2)[Rh(COD)]$ (**5**)	**D** (41)	22.7	89.3, 85.6	−4338
	E (59)	40.2	90.6, 87.8	−4357
$[Pt(C_6F_5)_3](\mu\text{-}PPhPy_2)[Rh(TFB)]$ (**6**)	**D** (64)	22.9	65.7, 67.7	−4333
	E (36)	36.5	63.5, 64.3	−4423
$[Pt(C_6F_5)_3](\mu\text{-}PPhPy_2)[Rh(CO)_2]$ (**3**)	**D** (100)	20.8		−4320
$(NBu_4)[Pt(C_6F_5)_3(PPhPy_2)]$ (**2**)		19.0		−4373
$[Pt(C_6F_5)_3](\mu\text{-}PPy_3)[Rh(COD)]$ (**7**)	**D** (45)	26.6	88.2, 87.7	−4362
	E (55)	40.8	90.3, 88.8, 86.2, 84.5	−4410
$[Pt(C_6F_5)_3](\mu\text{-}PPy_3)[Rh(TFB)]$ (**8**)	**D** (65)	25.90	67.3, 65.8	−4340
	E (35)	37.93	64.8	−4428
$[Pt(C_6F_5)_3](\mu\text{-}Ppy_3)[Rh(CO)_2]$ (**4**)	**D** (100)	20.59		−4314

Results

Complexes **1** and **2** were prepared according to eq 1, by substitution of tht by $PPhPy_2$ or PPy_3 on the precursor $(NBu_4)[Pt(C_6F_5)_3(tht)]$. The resulting compounds, **1** and **2** were used as anionic N,N ligands for cationic $[Rh(diolefin)(solv)_2]^+$ (solv = solvent) or $[Rh(CO)_2(solv)_2]^+$ complexes prepared in situ (eqs 2 and 3), affording zwitterionic Pt/Rh complexes **3**−**8**.

$$(NBu_4)[Pt(C_6F_5)_3(tht)] + PPy_nPh_{3-n} \rightarrow (NBu_4)[Pt(C_6F_5)_3(PPy_nPh_{3-n})] \quad (1)$$

$$n = 2, \mathbf{1}; n = 3, \mathbf{2}$$

$$(NBu_4)[Pt(C_6F_5)_3(PPy_nPh_{3-n})] + [Rh(CO)_2(solv)_2]NO_3 \rightarrow [Pt(C_6F_5)_3(\mu\text{-}PPy_nPh_{3-n})Rh(CO)_2] + (NBu_4)NO_3 \quad (2)$$

$$n = 2, \mathbf{3}; n = 3, \mathbf{4}$$

$$(NBu_4)[Pt(C_6F_5)_3(PPy_nPh_{3-n})] + [Rh(diolefin)(solv)_2]ClO_4 \rightarrow [Pt(C_6F_5)_3(\mu\text{-}PPy_nPh_{3-n})Rh(diolefin)] + (NBu_4)ClO_4 \quad (3)$$

diolefin = COD, $n = 2$, **5**, and $n = 3$, **7;**
diolefin = TFB, $n = 2$, **6**, and $n = 3$, **8**

Compounds with Only Geometry D: Complexes 3 and 4. The compounds $[Pt(C_6F_5)_3(\mu\text{-}PPy_nPh_{3-n})Rh(CO)_2]$ (n = 2, **3**; $n = 3$, **4**) have a structure **D** in solution, as evidenced by their NMR spectra (selected NMR data given in Table 2). The rotation of the C_6F_5 groups around the $M-C_{ipso}$ bond is hindered, as it is often found in other fluoroaryl complexes of square-planar Pd and Pt species.[5] In complexes **3** and **4** also the rotation around the P—Pt bond is restricted, probably due to the proximity of the coordination planes of Pt and Rh. Hence, the F^2 and F^6 atoms of each C_6F_5 are nonequivalent and give rise to four signals (2:2:1:1) in the ^{19}F NMR spectrum, two of double intensity for the two C_6F_5 cis to phosphorus and two for the C_6F_5 trans to phosphorus (Figure 1). On the other hand, the pendant ring of the PPy_nPh_{3-n} ligand (Ph in $PPhPy_2$ or the noncoordinated Py in PPy_3) is sandwiched between the two coordinated Py rings. Accordingly the ^1H and ^{13}C NMR spectra of **3** show five signals for the five inequivalent C−H groups of the Ph ring. For **4** a further consequence of this location is that the noncoordinated Py group is unable to undergo fast exchange with those coordinated to rhodium, and distinct and sharp signals for the pendant and the coordinated Py groups are observed in the ^1H NMR spectrum at 25 °C. The exchange between coordinated and noncoordinated Py groups is slow on the NMR time scale.

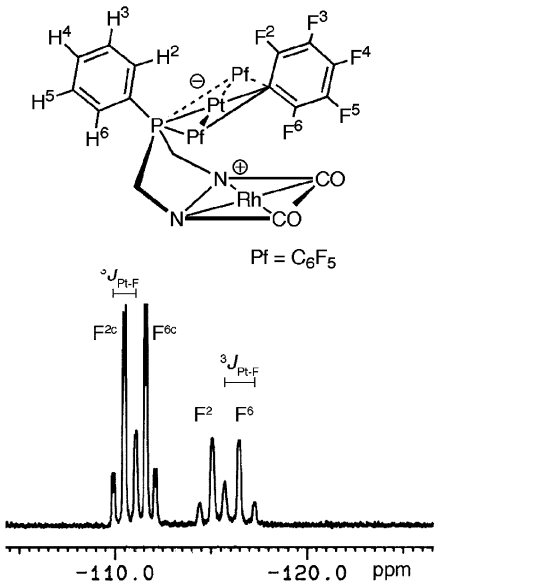

Figure 1. Structure and ^{19}F NMR spectrum (only F_{ortho}) of complex **3** showing the inequivalence of the fluorine atoms of the C_6F_5 ligands and the protons of the phenyl ring. For clarity only one C_6F_5 group is shown. F^2 and F^6 signals correspond to the C_6F_5 group trans to phosphorus, while F^{2c} and F^{6c} signals correspond to the two equivalent C_6F_5 groups cis to phosphorus.

In the cases of carbonyl compounds, the CO stretching can be used as an additional indicator of the coordination mode. It is known that pentacoordinated $[MTp'(CO)_2]$ complexes show the two stretching vibrations (symmetrical and asymmetrical) at lower energy compared to their four-coordinated isomers.[9] Since the values obtained for the CO stretching in complexes **3** and **4** are very close, both of them are assigned a square-planar coordination (the only one possible for **3**). This eliminates structure **F** for **4**.

Compounds with Geometries D and E Coexisting: Complexes 5, 6 and 7, 8. Complexes of the type $[(C_6F_5)_3Pt(\mu\text{-}PPy_nPh_{3-n})Rh(diolefin)]$ give in solution a mixture of isomers **D** and **E** (Chart 1) which do not interconvert on the NMR time scale. The major isomer is **E** for diolefin = COD but **D** for diolefin = TFB (Table 2). The spectroscopic

(20) *International Tables for Crystallography*; Kluwer: Dordrecht, The Netherlands, 1992; Vol. C.

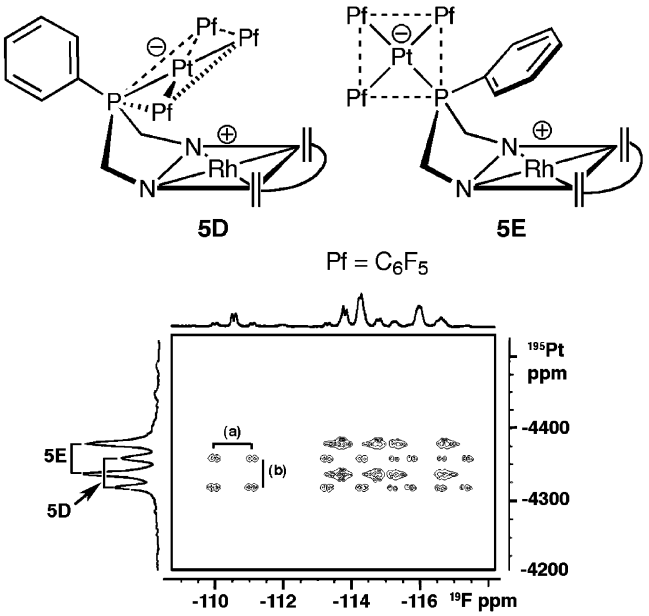

Figure 2. $^{19}F-^{195}Pt$ correlation experiment of **5** at room temperature. The cross-peaks correlate each signal of ^{195}Pt with the satellites of the signals on the ^{19}F spectrum: (a) = $^3J_{^{19}F-^{195}Pt}$; (b) = $^1J_{^{31}P-^{195}Pt}$. Only the F_{ortho} signals (F^2 and F^6) have been recorded.

properties (^{19}F and ^1H NMR) of isomers **D** are similar to those described above for compounds **3** and **4** and are not further discussed here. The isomers **E** give in the ^{19}F NMR at room temperature only two signals (2:1) due to the F_{ortho} atoms because in this geometry there is fast rotation about the P—Pt bond, which makes equivalent the four F_{ortho} nuclei of the two C_6F_5 groups cis to phosphorus as well as the F^2 and F^6 nuclei on the C_6F_5 group trans to phosphorus. In all the complexes studied these signals appear partially overlapped with the signals of F_{ortho} nuclei of the **D** isomer and with their satellites due to $^{19}F-^{195}Pt$ coupling. However all the signals are easily identified in $^{19}F-^{195}Pt$ correlation experiments (see for instance Figure 2 for complex **5**).

Due to the symmetry of the complexes, in the isomers **5E** and **6E** four of the five ^1H nuclei of the phenyl ring are equivalent by pairs, and only three cross-peaks are obtained in the $^1H-^{13}C$ experiment. With PPy_3 (complexes **7E** and **8E**) the asymmetry of the noncoordinated Py group, which lies above the coordination plane (see Figure 2), lowers the symmetry of the complex leading, in the slow-exchange limit, to chemical nonequivalence of the two coordinated Py groups and the four olefinic hydrogens. In fact this is the spectrum obtained for **7E** at 193 K. At higher temperatures the fast exchange of the coordinated Py groups with the pendant one renders the three rings equivalent and also the four olefinic hydrogens. For **8E** the exchange of Py groups is very fast and the coalescence temperature is below the 193 K limit reached in our study.

It is known for Tp′Rh−olefin complexes that κ^3-Tp′ compounds display the olefinic carbon signal at higher field than their κ^2-Tp′ analogues.[9b,21] A similar effect should be expected here, but the olefinic carbon signals of the complexes with PPy_3 do not show any relevant shift with respect to those with $PPhPy_2$. Hence, although the ^1H spectrum of **8D** could be misinterpreted as being the result of a pentacoordinated complex, the ^{13}C spectrum clearly supports a square planar coordination (Table 2). Thus, the spectroscopic data show no evidence for structures of the type **F** in the complexes with the ligand $[(C_6F_5)_3Pt(\mu\text{-}PPy_3)]^-$. This is in contrast with the usual behavior of $[RBpz_3]^-$ ligands.

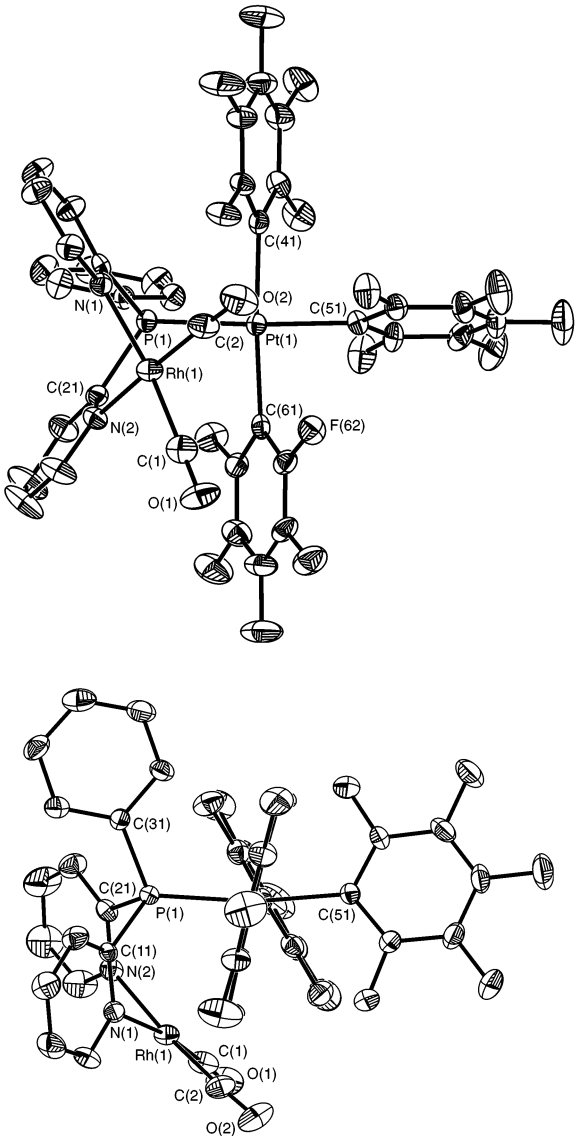

Figure 3. Two ORTEP plots of **4D**·0.5hex with thermal ellipsoids drawn at the 30% probability level.

X-ray Structures of Complexes 4D·0.5hex and 5E·2(CD$_3$)$_2$CO. The two structural types proposed from spectroscopic studies have been confirmed in the solid state for representative complexes.

The X-ray diffraction structure of **4D**·0.5hex is shown in Figure 3. Distances and angles at the coordination planes of the two metals are gathered in Table 3. The structure strongly suggests that the molecule is distorted to bring close the rhodium and the platinum coordination planes in a **D**-type geometry. The angles C(61)−Pt(1)−P(1) and Pt(1)−P(1)−C(21) have values of 94.2 and 119.4°, respectively, and the

(21) Del Ministro, E.; Renn, O.; Rüegger, H.; Venanzi, L. M.; Burckhardt, U.; Gramlich, V. *Inorg. Chim. Acta* **1995**, *240*, 631.

Table 3. X-ray Structural Data: Selected Distances (Å) and Angles (deg)

4D·0.5hex		**5E**·2$(CD_3)_2CO$	
Rh(1)−N(1)	2.095(5)	Rh(1)−N(1)	2.108(8)
Rh(1)−N(2)	2.082(6)	Rh(1)−N(2)	2.121(8)
Rh(1)−C(1)	1.875(9)	Rh(1)−M(1)[a]	2.027(17)
Rh(1)−C(2)	1.848(10)	Rh(1)−M(2)[a]	2.021(16)
Rh(1)−Pt(1)	3.590(2)	Rh(1)−Pt(1)	5.687(2)
P(1)−Pt(1)	2.254(2)	P(1)−Pt(1)	2.281(3)
P(1)−Rh(1)	3.197(2)	P(1)−Rh(1)	3.432(3)
Pt(1)−C(41)	2.082(6)	Pt(1)−C(41)	2.069(10)
Pt(1)−C(61)	2.082(7)	Pt(1)−C(61)	2.053(11)
Pt(1)−C(51)	2.056(7)	Pt(1)−C(51)	2.069(9)
N(1)−Rh(1)−N(2)	86.0(2)	N(1)−Rh(1)−N(2)	88.4(2)
C(41)−Pt(1)−C(51)	87.6(3)	C(41)−Pt(1)−C(61)	85.8(4)
C(61)−Pt(1)−C(51)	88.6(3)	C(61)−Pt(1)−C(51)	87.3(4)
C(41)−Pt(1)−P(1)	89.5(2)	C(41)−Pt(1)−P(1)	95.5(3)
C(61)−Pt(1)−P(1)	94.2(2)	C(51)−Pt(1)−P(1)	91.3(3)

[a] M(1) and M(2) are the C(1)−C(2) and C(3)−C(4) centroids.

P(1) atom is situated 0.333 Å above the plane defined by the other three donor atoms (C(41), C(51), and C(61)) and the Pt(1) atom. The Pt atom is not on the normal to the rhodium coordination plane passing through the Rh center but displaced to one side. At the same time the fluoroaryl rings are tilted with respect to the coordination plane at the Pt atom, with angles in the range 60−76°. One of them (C(61)−C(66)) makes an angle of only 18.8° with the rhodium coordination plane, which allows the rhodium to reduce the steric hindrance by approaching this pentafluorophenyl ring (the shortest nonbonding distance to the atoms of this ring is Rh(1)···F(62) of 3.561 Å) and moving away from the opposed fluoroaryl ring C(41)−C(46) (the shortest nonbonding distance to the atoms of this ring is Rh(1)···F(42) of 3.538 Å). Therefore, the shortest distances between the rhodium atom and the platinum frame are Rh(1)···F(42) and Rh(1)···F(62). There is also a tetrahedral distortion in the rhodium frame, being the angle between the planes N(1)-Rh(1)N(2) and C(1)Rh(1)C(2) of 9.8°, to avoid a contact distance between the carbonyl group C(1)O(1) and the closest fluoroaryl ring. These features lead to a Pt(1)−Rh(1) distance of 3.590 Å, still too large to consider a interaction between the metal centers but lower than in an undistorted geometry.

Finally, the phenyl ring C(31)−C(36) bisects the angle formed by the pyridyl rings. This situation hinders its rotation about the C−P bond, in agreement with the NMR observation discussed above.

The X-ray diffraction structure of **5E**·2$(CD_3)_2CO$ is shown in Figure 4, with distances and angles at the coordination planes of the two metals collected in Table 3. The structure shows that the coordination about each metal is slightly distorted square planar, with both coordination planes roughly perpendicular (with an angle between them of 119°). The aryl ring on the P atom is lying over the Rh coordination plane and is almost parallel to the nearest fluorophenyl ring. All the bond lengths and angles are within the normal values, and the fluoroaryl rings are tilted with respect to the Pt coordination plane with angles in the range 67−77°.

The main deviation from the ideal geometry in the Pt is due to the value of the C(41)−Pt(1)−P(1) angle (95.5°)

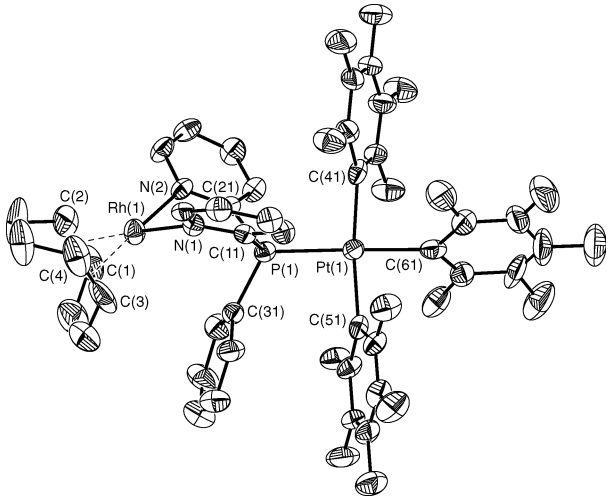

Figure 4. ORTEP plot of **5E**·2$(CD_3)_2CO$ with thermal ellipsoids drawn at the 30% probability level.

Scheme 1

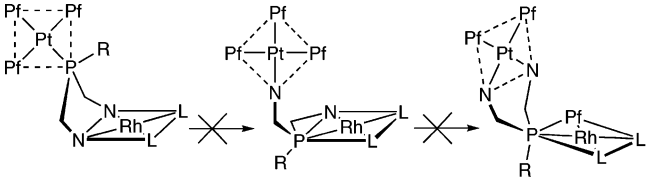

imposed by the steric hindrance between the $PPhPy_2$ ligand and the fluoroaryl ring. In the Rh center the $PPhPy_2$ ligand behaves as an N,N donor ligand, with the phenyl ring oriented toward the Rh in an **E**-type geometry. The Pt and Rh centers are separated by more than 5 Å. This configuration of the chelate ring is also found in some X-ray structures of Pd, Pt, and Rh complexes with 2-pyridylphosphine oxides as ligands.[5] Geometry **E** is also found in the solid state for Tp′Rh derivatives.[6,9,22]

Discussion

Pyridylphosphine ligands allow the easy and controlled synthesis of bimetallic complexes. The phosphorus is first coordinated to Pt affording a metal-containing N,N donor chelate, which is then coordinated to a Rh(I) center. Although the P,N-chelating coordination of other P,N ligands to transition metal centers (including Rh) is well documented,[1,14] apparently the P,N chelation on rhodium does not compete with the observed N,N chelation in complexes **5** and **4** (Scheme 1). In other words, the regiochemistry is mostly controlled by the ring size of the resulting metalacycle. A four-membered P,N chelate should be unfavorable versus a six-membered N,N chelate. The other possible structure shown in Scheme 1, which involves transmetalation of a C_6F_5 group, is not observed either.

Stereochemistry at the Phosphorus: Isomer D vs Isomer E. As described above, complexes **4** and **5** are square planar in solution. Two geometries are possible depending

(22) See for instance: (a) Akita, M.; Ohta, K.; Takahasi, Y.; Hikichi, S.; Moro-Oka, Y. *Organometallics* **1997**, *16*, 4121. (b) Cocivera, M.; Desmond, T. J.; Ferguson, G.; Kaitner, B.; Lalor, F. J.; O'Sullivan D. J. *Organometallics* **1982**, *1*, 1125−1132.

Chart 2

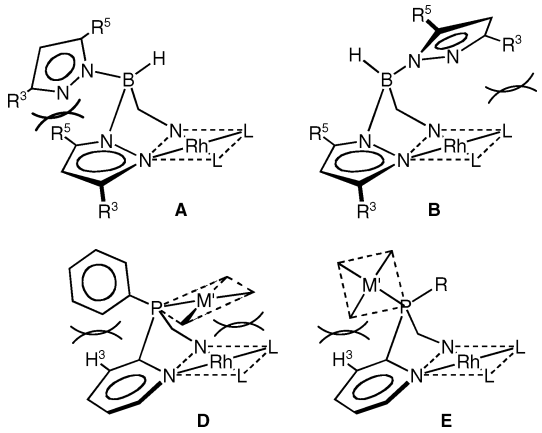

on the relative distribution of the substituents on the phosphorus: **D** if the third aryl ring is in a "pseudoequatorial" position (toward the rhodium center) or **E** if the noncoordinated aryl is in a "pseudoaxial" position (away from the rhodium center, Chart 1).

The discrimination of the solution structures **D** and **E** is straightforward considering the differences in their dynamic behavior. Complexes with the **D** structure are quite static in solution. At 25 °C they do not undergo fast rotation about the Pt−P or Pt−C bonds and each pentafluorophenyl ring gives five signals in their ^{19}F NMR spectra. The rotation about the P−C(phenyl) bond in complexes with $PPhPy_2$ is also hindered, due to the location of the phenyl ring between the coordinated pyridyl groups, and five signals are obtained in the ^{1}H−^{13}C HMQC spectrum. On the contrary, in complexes **E**, the rotations about Pt−P and P−C(phenyl) are not hindered and only three ^{19}F signals from the C_6F_5 trans to P plus three more ^{19}F signals from the two equivalent C_6F_5 groups cis to P are observed. Also, only three signals arising from C(phenyl)−H are obtained in the HMQC spectrum of complexes with $PPhPy_2$.

In previous works we have studied the behavior of P-blocked $EPPhPy_2$ and $EPPy_3$ derivatives (E = O, S) in which the phosphorus atom has been oxidized and the two Py rings behave as a chelate in square-planar complexes.[5] The geometry found was always **E**. On the other hand, the stereochemistry in "boatlike" metallacycles has been analyzed for complexes with pyrazolylborates (Chart 2). Bulky R^5 substituents produce steric repulsion between these and the free Pz ring in conformation **A**, favoring conformation **B**. A coordination environment crowded out of the coordination plane of the metal repels the noncoordinated Pz ring in **B**, favoring conformation **A**.[9,10,23]

In 2-pyridylphosphine complexes with the phosphorus coordinated to $[Pt(C_6F_5)_3]^-$ the biggest steric interactions of the Rh ligands are with the platinum complex, more than with the other phosphorus substituent (Ph or Py). Considering other intramolecular interactions it was, however, difficult to decide a priori whether the overall steric hindrance was bigger in conformation **D** or in **E**. It must also be taken into account that the anionic charge on the platinum moiety (probably distributed mostly between the Pt−C and the C−F bonds) can introduce a term of attractive electrostatic interaction with the rhodium (positive) fragment in favor of conformation **D**. The experimental results suggest that the preferred conformation depends much on the steric requirements of the ligands on the rhodium center above the coordination plane. For small size ligands lying in the coordination plane, such CO in **3** and **4**, conformation **D** is preferred since the $[Pt(C_6F_5)_3]^-$ plane can be located over the Rh plane, bringing regions with opposite electrostatic charge closer to each other. In this geometry, the rotation around the P−Pt bond is very hindered. In fact, a putative rotation intermediate, in which both coordination planes are perpendicular, would push the platinum group to an equatorial location, which means close to conformation **E**, producing an exchange between **D** and **E**. The fact that this is not observed suggests a noticeable difference in stability in favor of **D** in this case.

Conformational Exchange. This conformational exchange, although slow, is observed on the NMR time scale for complexes with COD, as a result of the destabilization of **D** when the ligands on Rh invade the space above its coordination plane. The exchange is faster for the complexes with TFB, **6** and **8**, which show the coalescence of the P signals assigned to both conformers at room temperature. This dependence of the rate of conformational exchange on the olefin coordinated to the rhodium must be the result of two factors associated with the geometry of the TFB ligand: (i) a larger destabilization of the ground state due to the bigger steric repulsion of the TFB with the P axial subtituents; (ii) a stabilization of the transition state for the TFB complex with respect to the COD complexes, due to the smaller bite angle of the former and therefore the smaller interaction between the olefinic bond and the H^6 of the Py coordinated to the rhodium in a putative planar transition state.

Py Exchange. Complexes **6E** and **8E** have a structure similar to that of **5** in the solid state (Figure 2), with an uncoordinated pyridyl group in place of the phenyl ring. This orientation facilitates the substitution of coordinated Py by pendant Py groups. For **8E** this exchange is fast at 193 K, rendering spectroscopically equivalent the three Py rings and the four olefinic protons. For **6E** the exchange of Py and also the rotation of the Py ring about the P−C bond are slow at 193 K. Both processes share their coalescence in the NMR spectra, suggesting a common transition state with the incoming Py plane lying perpendicular to the rhodium coordination plane. For analogous complexes of Pd(II) and Rh(I) with Py_3PO, the rotation of the uncoordinated Py is too fast to be detected by NMR.[5,17] An important consequence of conformation **D** is the inability of the third Py ring to substitute the coordinated Py groups in the rhodium center. In fact this chemical exchange is very slow for **4D** and does not affect the shape of their NMR spectra at 25 °C.

In summary, the Py exchange is very fast in complexes **E** and is controlled by the conformational exchange in com-

(23) Akita, M.; Hashimoto, M.; Hikichi, S.; Moro-oka, Y. *Organometallics* **2000**, *19*, 3744−3747.

Table 4. CO Stretching Frequencies for Neutral and Cationic Square-Planar Dicarbonylrhodium(I) Complexes

complex	ν(CO) (cm^{-1})	solvent	ref
$[Pt(C_6F_5)(\mu\text{-}PPhPy_2)Rh(CO)_2]$ (**3**)	2103, 2044	CH_2Cl_2	this work
$[Pt(C_6F_5)(\mu\text{-}PPy_3)Rh(CO)_2]$ (**4**)	2102, 2044	CH_2Cl_2	this work
$[RhTp^{Ph,Me}(CO)_2]$ (two conformers)	2089, 2022	$CHCl_3$	24b
	2077, 2008		
$[RhTp^{Me}(CO)_2]$	2085, 2019	$CHCl_3$	25
$[RhTp^{iPr,4Br}(CO)_2]$ (two conformers)	2089, 2026	$CHCl_3$	25
	2077, 2020		
$[Rh(Pz_4B)(CO)_2]$	2088, 2022	hexane	26
$[Rh(OPPy_2Ph)(CO)_2]^+$	2104, 2047	CH_2Cl_2	5d
$[Rh(PMI)(CO)_2]^+$ [a]	2102, 2042	CH_3CN	27
$[Rh(PEI)(CO)_2]^+$ [b]	2101, 2042	CH_3CN	27
$[Rh(PiPI)(CO)_2]^+$ [c]	2100, 2039	CH_3CN	27
$[Rh(bipy)_2(CO)_2]^+$	2108, 2050	Nujol mull	28
$[\{(3,5\text{-}Me_2Pz)_2CH_2)\}Rh(CO)_2]^+$	2100, 2035	Nujol mull	24c

[a] PMI = 2-pyridinalmethylimine. [b] PEI = 2-pyridinalethylimine. [c] PiPI = 2-pyridinalisopropylimine.

plexes **D**, a behavior comparable to that of analogous compounds with pyrazolylborate ligands.[8,9]

Differences of the N-Donor Ends in $[HBPz_3]^-$ and in $[(C_6F_5)_3Pt(\mu\text{-}PPy_nPh_{3-n})]^-$ Ligands. The stretching CO band in the IR spectra shows no observable effect of the negative charge of the $[(C_6F_5)_3Pt(\mu\text{-}PPy_nPh_{3-n})]^-$ ligands on the rhodium center, since the observed values are similar to those obtained for cationic dicarbonyl complexes such as $[Rh(CO)_2(OPPy_nPh_{3-n})]^+$ and much higher than for complexes with anionic $[HBPz_3]^-$ ligands.[9,24] Table 4 gathers ν(CO) values for representative cationic and neutral complexes with N,N chelated ligands. Only values for square-planar isomers are collected, and complexes with donor groups very different from Py or Pz have been excluded. Complexes **3** and **4** show ν(CO) wavenumbers in the range found for cationic complexes with neutral ligands, tipically ν_{sym} about 2100 cm^{-1} and ν_{ass} about 2040 cm^{-1}. Neutral complexes show ν_{sym} about 2085 cm^{-1} and ν_{ass} about 2025 cm^{-1}. This suggests that the electron density of the negative charge is mostly delocalized in the $(C_6F_5)_3Pt$ fragment for $[(C_6F_5)_3Pt(\mu\text{-}PPy_nPh_{3-n})]^-$ ligands, as proposed above in the structure discussion) while it is more delocalized in the pyrazolate rings for $[HBPz_3]^-$. Consequently the latter are much better N,N donors.

Conclusion

In conclusion, the conformational and dynamic behavior of anionic $[(C_6F_5)_3Pt(\mu\text{-}PPy_nPh_{3-n})]^-$ ligands is comparable to that of Tp′, but conformation **D** is more favorable in the former due to the bulkiness of the $(C_6F_5)_3Pt$ moiety and its negative charge. On the other hand, the Tp′ ligands are much better N,N donors than $[(C_6F_5)_3Pt(\mu\text{-}PPy_nPh_{3-n})]^-$. These features disfavor the κ^3 coordination mode, which has not been found for $[(C_6F_5)_3Pt(\mu\text{-}PPy_3)]^-$ ligands although it is frequent for Tp′ rhodium complexes.

Acknowledgment. Financial support by the Ministerio de Ciencia y Tecnología (Project BQU2001-2015) and the Junta de Castilla y León (Project No. VA120-01) is very gratefully acknowledged.

Supporting Information Available: Crystallographic data in CIF format. This material is available free of charge via the Internet at http://pubs.acs.org.

IC034863F

(24) (a) Burling, S.; Field, L. D.; Messerle, B. A. *Organometallics* **2000**, *19*, 87−90. (b) Moszner, M.; Woloviec, S.; Trösch, A.; Heinrich, V. *J. Organomet. Chem.* **2000**, *595*, 178−185. (c) Oro, L. A.; Esteban, M.; Claramunt, R. M.; Elguero, J.; Foces-Foces, C.; Cano, F. H.; *J. Organomet. Chem.* **1984**, *276*, 79−97.

(25) Bucher, U. E.; Currao, A.; Nesper, R.; Rüegger, H.; Venanzi, L. M.; Younger, E. *Inorg. Chem.* **1995**, *34*, 66−74.

(26) King, R. B.; Bond, A. *J. Organomet. Chem.* **1974**, *73*, 115.

(27) Zassinovich, G.; Camus, A.; Mestroni, G. *J. Organomet. Chem.* **1977**, *133*, 377−384.

(28) Reddy, G.; Susheelemma, L. *Chem. Commun.* **1970**, 54.